This article has been accepted for publication in a future issue of this journal, but has not been fully edited. Content may change prior to final publication. Citation information: DOI 10.1109/JESTPE.2015.2478149, IEEE Journal of Emerging and Selected Topics in Power Electronics

An Active Filter with Resonant Current Control to Suppress Harmonic Resonance in a Distribution Power System

Tzung-Lin Lee, *Member, IEEE,* Shang-Hung Hu, *Student Member, IEEE,*

***Abstract*—A shunt active filter operated as a harmonic conductance is able to suppress harmonic resonance in the distribution power system. However, due to the inherent phase lagging in digital-signal processing, the active filter really behaves as a harmonic admittance instead of conductance. This may induce unintentional harmonic amplification at other locations in the feeder when starting the active filter, which is similar to the so-called "whack-a-mole" phenomenon. This paper presents an active filter with resonant current control to suppress harmonic resonance. The current control is realized by parallel-connected band-pass filters tuned at harmonic frequencies to ensure that the active filter functions as an approximately pure conductance. The conductance at dominant harmonic frequencies can be separately and dynamically adjusted to guarantee the damping performance. In addition, in order to address the harmonic resonance, the line distributed-parameter model of a radial feeder is developed with considering harmonic damping by variable conductance and admittance, respectively. Simulation results show that the active filter with the resonant control provides better damping performance compared with other control methods. A lab-scale prototype circuit rated at 220V/20kVA also validates the effectiveness of the proposed method.**

KEYWORDS

Active filter, resonant current control, harmonic resonance

I. INTRODUCTION

Voltage distortion, due to harmonic resonance between power factor correction capacitors and line inductors, has received serious concerns in the distribution power system [1], [2], [3], [4], [5], [6]. This scenario becomes significant due to extensive use of nonlinear loads as well as high penetration of inverter-based distributed generation systems [7]. According to IEEE std. 519-1992 [8], maximum allowable voltage total harmonic distortion (THD) is 5% and individual voltage distortion is 3% in distribution networks below 69kV. This guideline is also included in IEEE standard for interconnecting distributed resources with electric power systems (IEEE std. 1547.2-2008). Tuned-passive filters are typically adopted to cope with harmonic issues, but their functionality may suffer from component aging, frequency shifting, or unintentional resonances. Therefore, engineering calibration on passive filters is frequently required to maintain their filtering performances.

This work was supported by Ministry of Science and Technology of TAIWAN under grant 104-2221-E-110-037.

Tzung-Lin Lee and Shang-Hung Hu are with the Department of Electrical Engineering, National Sun Yat-sen University, Kaohsiung 80424, TAIWAN, (e-mail: tllee@mail.ee.nsysu.edu.tw; rabbit17212@hotmail.com).

The shunt active filter controlled as a fixed or variable conductance has been proposed to suppress harmonic resonances in a radial power distribution system [9]. The mismatching between the conductance of active filter and the characteristic impedance of the line may result in unintentional amplification of harmonics due to the harmonic standing waves. This phenomenon is analogous to a "whack-a-mole" amusement for children [10]. As soon as a child whacks a mole appearing from a hole, the mole goes back into the hole. Another mole immediately appears from another hole and this activity is repeated endlessly. Thus voltage harmonics can be well dampened at the installation point of the filter, whereas unintentional harmonic resonances may be excited in the other location of the feeder with no filter installed. In order to approach this issue, a real-time communication system [11], [12] was proposed to coordinate operation of distributed active filters by using droop-control [13], on-line optimization [14], [15], particle swarm optimization [16] or single-frequency tuned algorithm [17]. In a nutshell, the active filter working as harmonic conductance is able to suppress the propagation of harmonic voltage on the feeder. However, instead of conductance, the active filter presents inductive characteristic at harmonic frequencies due to the limited bandwidth of the current control [18]. The phase lagging may be further worsen by the controlling delay of the active filter in the digital system. Thus the harmonic admittance deteriorates the damping performance of the active filter, or even result in revival of the "whack-a-mole" issue.

Various current control methods have been proposed for active power filters. Hysteresis current regulator is simplest, but low-order harmonics resulting from variable switching frequency may become a serious concern [19]. Repetitive control with selectively harmonic compensation is very popular. However, this approach may suffer from heavy computing loading [20]. A shunt active filter with asymmetrical predictive current control was presented for harmonic-resonance suppression in the power system [21], [18], [22]. In this application, current-tracking capability is very sensitive to parameter variations. Analysis of stability margin of the active filter was discussed in [18]. Recently, resonant controls have been applied for the active power filters. Most of research was simply focused on harmonic current compensating at load side [23], [24], [25], [26], [27], [28].

In the previous work, the authors has presented the resonant current control for the shunt active power filter to dampen harmonic voltage propagation[29]. The resonant current regulator

This article has been accepted for publication in a future issue of this journal, but has not been fully edited. Content may change prior to final publication. Citation information: DOI 10.1109/JESTPE.2015.2478149, IEEE Journal of Emerging and Selected Topics in Power Electronics

is composed of various parallel-connected band-pass filters tuned at harmonic frequencies to control the active filter as an approximately pure conductance [30], [31]. The conductance of each harmonic frequency is designed to be separately and dynamically adjusted to guarantee the damping performance. In this study, the impact of phase lagging on harmonic damping performance is further investigated by using the line distribution-parameter model. Damping performance of the active filter is also analyzed when different current controls are implemented and when nonlinear loads are deployed at different locations. Experimental results from a prototype circuit based on 220V/10kVA system verify theoretical analysis.

This paper is organized as follows. Operation principle of the active filter with the resonant current control is presented in Section II. In Section III, the the impact of harmonic admittance on harmonic resonance is analyzed, including the "whack-a-mole" issue. Supporting results from simulation studies and experimental tests are provided in Section IV and V to validate the effectiveness. Finally, Section VI gives the conclusion.

II. Operation principle

A simplified one-line circuit diagram of the proposed active filter and the associated control are shown in Fig. 1. The active filter unit (AFU) is installed at the end of a radial line to suppress harmonic resonance. The AFU operates as a variable conductance for different harmonic frequency as given,

$$i^*_{abc,h} = \sum_h G^*_h \cdot E_{abc,h} \tag{1}$$

where h represents the order of the harmonic frequency. The conductance command G^*_h is defined as a control gain to dampen harmonic voltage $E_{abc,h}$. As shown in Fig. 1, the control is composed of harmonic-voltage extraction and tuning control, followed by the current regulation and PWM algorithm. Operation principle and design consideration are given as follows.

A. AFU control

Harmonic voltage at the different frequency is determined based on the so-called synchronous reference frame (SRF) transformation. The specific harmonic voltage component becomes a dc value after E_{abc} is transformed into the SRF at ω_h, Accordingly, a low-pass filter (LPF) is applied to separate the dc value and then the corresponding harmonic component $E_{abc,h}$ is obtained when applying reverse transformation. It is worth noting here that a phase-locked loop (PLL) is required to determine system frequency for implementation of SRF. ω_h should be set as a negative value for negative-sequence component (i.e., fifth) or a positive value for positive-sequence harmonic component (i.e., seventh), respectively.

Fig. 2 shows the tuning control for the conductance command G^*_h. As illustrated, G^*_h is determined according to the harmonic voltage distortion VD_h at the AFU installation point E_{abc}, in which VD_h is defined as the percentage ratio of the harmonic voltage component E_h (rms value) to the voltage E (rms value) by

$$\begin{aligned}
\mathrm{VD}_h &= \frac{E_{h,RMS}}{E_{RMS}} \cdot 100\% \\
E_{h,RMS} &= \sqrt{\frac{\int_t^{t+T} (E_{a,h}(t)^2 + E_{b,h}(t)^2 + E_{c,h}(t)^2)}{T} dt} \\
E_{RMS} &= \sqrt{\frac{\int_t^{t+T} (E_a(t)^2 + E_b(t)^2 + E_c(t)^2)}{T} dt}.
\end{aligned} \tag{2}$$

The derivation of VD_h is approximately evaluated by using two LPFs with cut-off frequency at ω_c, which are to filter out ripple components in the calculation. The error between the allowable harmonic voltage distortion VD^*_h and the actual harmonic voltage distortion VD_h is then fed into a proportional-integral (PI) regulator to adjust the conductance command G^*_h. Hence, a variable conductance command G^*_h for the different harmonic frequency is generated.

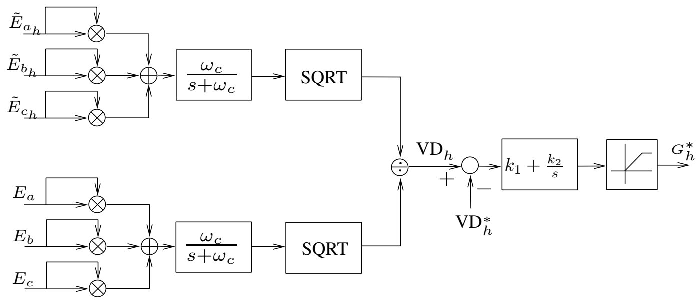

Fig. 2. Tuning control of the conductance command.

The total current command is the summation of fundamental current command $i^*_{abc,f}$ and all harmonic current commands $i^*_{abc,h}$, which is equal to the product of the harmonic voltage and its corresponding conductance command. $i^*_{abc,f}$ shown in Fig. 1 is the in-phase fundamental current command generated by a PI control to control the dc voltage V_{dc} of the AFU. In order for the active filter to guarantee current tracking capability, the resonant current regulator is realized by:

$$T_r(s) = k_p + \sum_h \frac{2K_{i,h}\xi\omega_h s}{s^2 + 2\xi\omega_h s + \omega_h^2} \tag{3}$$

where k_p is a proportional gain and $k_{i,h}$ is an integral gain for individual harmonic frequency, respectively. The current control is tuned to resonate at harmonic frequencies ω_h, so that various narrow gain peaks centered at harmonic frequencies are introduced. The damping ratio ξ is designed to determine the selectivity and bandwidth of the current control. Accordingly, the voltage command v^*_{abc} is obtained for PWM to synthesize the output voltage of the active filter.

B. Modelling of control

Nomenclature used in this section is given as:
$V_{sh}(s)$: harmonic voltage at the source terminal
$E_h(s)$: harmonic voltage at the installation location of the active filter
$I_h(s)$: harmonic current of the active filter

This article has been accepted for publication in a future issue of this journal, but has not been fully edited. Content may change prior to final publication. Citation information: DOI 10.1109/JESTPE.2015.2478149, IEEE Journal of Emerging and Selected Topics in Power Electronics

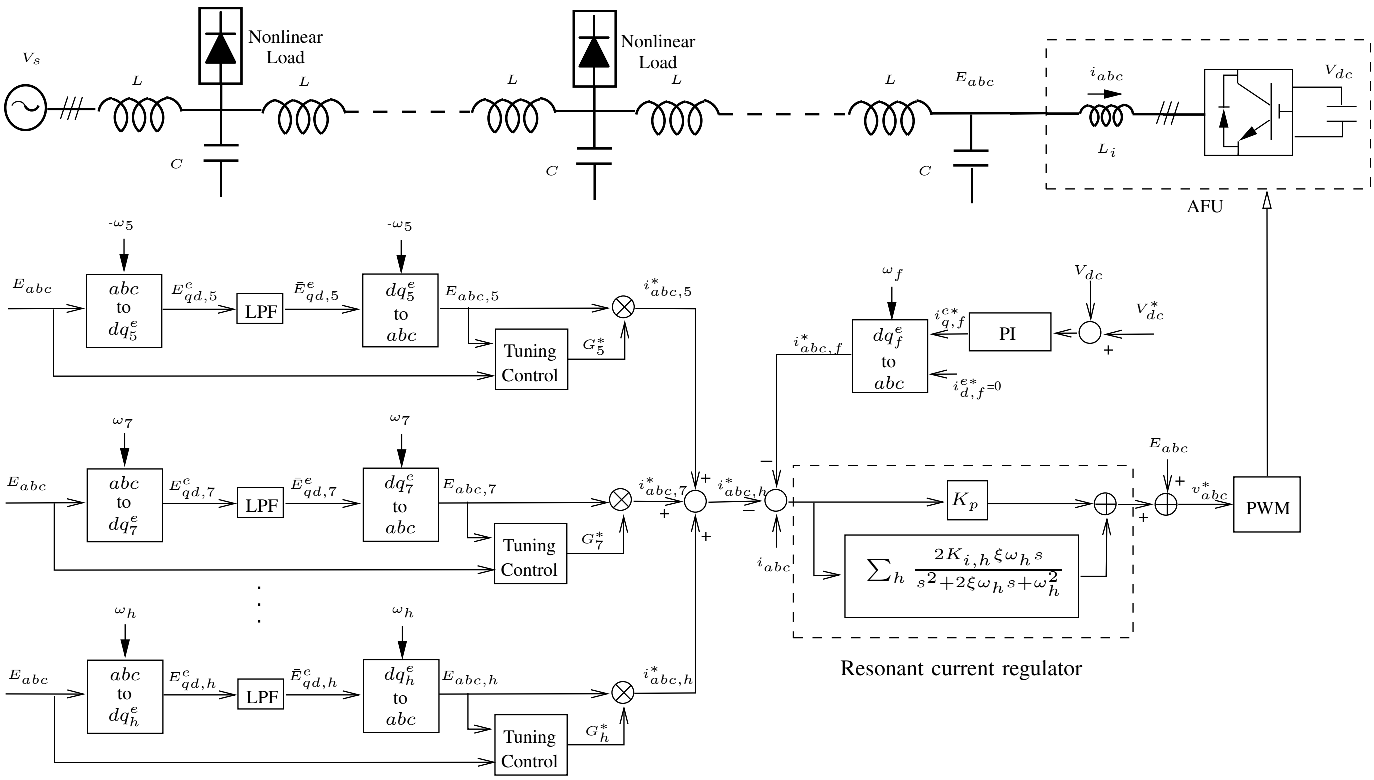

Fig. 1. Active filter and the associated control.

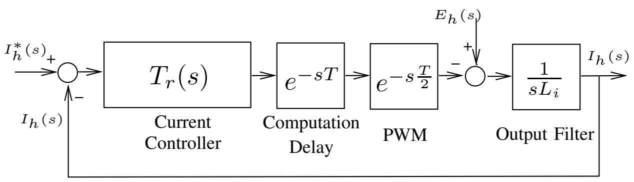

Fig. 3. Current control block diagram of the proposed AFU.

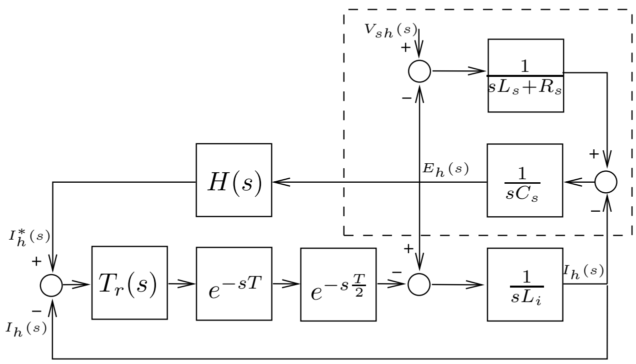

Fig. 4. Voltage control block diagram of the proposed AFU in the distributed power system.

$I_h^*(s)$: harmonic current command of the active filter

Fig. 3 shows current control block diagram for each phase. Digital signal processing delay and PWM delay are included, where T represents a sampling period. Hence, current loop stability and current tracking capability can be simply evaluated by using bode plots of open-loop and closed-loop transfer functions. Fig. 4 shows the block diagram for harmonic damping analysis. Since high-order harmonics seldom excite resonances, the distribution network is replaced with a second-order resonant tank (L_s, C_s, R_s) as indicated by the dashed-box. Here, the resonant tank is tuned to amplify the harmonic voltage $E_h(s)$. Note that the scheme of harmonic detection at ω_h is equivalent to a single-side bandpass filter in the stationary frame. The transfer function $H(s)$ can be expressed as (4), where ω_h is the harmonic frequency and T_{LPF} is time constant of the low-pass filter, which is used to filter out the dc component in the rotational reference frames. Thus the damping performance of the AFU can be evaluated by the harmonic-voltage magnification $\frac{|E_h(s)|}{|V_{sh}(s)|}$ shown in Fig. 4.

$$H(s) = G_h^* \frac{(s - j\omega_h)T_{LPF}}{1 + (s - j\omega_h)T_{LPF}} \tag{4}$$

TABLE I
PARAMETERS OF A GIVEN POWER LINE.

Line voltage	$11.4\,\mathrm{kV}$
Line frequency	$60\,\mathrm{Hz}$
Feeder length	$9\,km$
Line inductor	$1.55\,\mathrm{mH}/km (4.5\,\%)$
Line resistor	$0.36\,\Omega/km (1.2\,\%)$
Line capacitor	$22.7\,\mu\mathrm{F}/km (11.1\,\%)$
Characteristic impedance, Z_o	$8.45\,\Omega$
Wavelength of 5^{th} harmonics, λ_5	$17.8\,km$
Wavelength of 7^{th} harmonics, λ_7	$12.7\,km$
	3ϕ $11.4\,\mathrm{kV}$ $10\,\mathrm{MVA}$ base

This article has been accepted for publication in a future issue of this journal, but has not been fully edited. Content may change prior to final publication. Citation information: DOI 10.1109/JESTPE.2015.2478149, IEEE Journal of Emerging and Selected Topics in Power Electronics

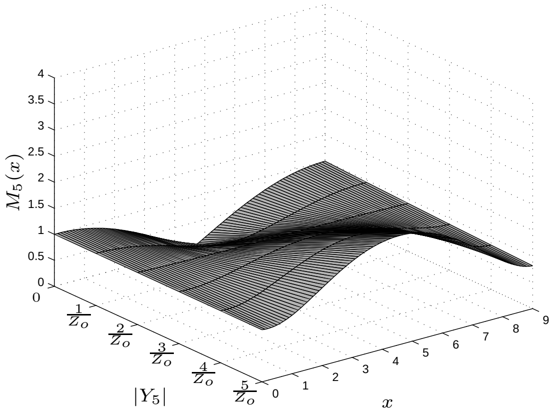

(a) The magnifying factor of the fifth harmonic.

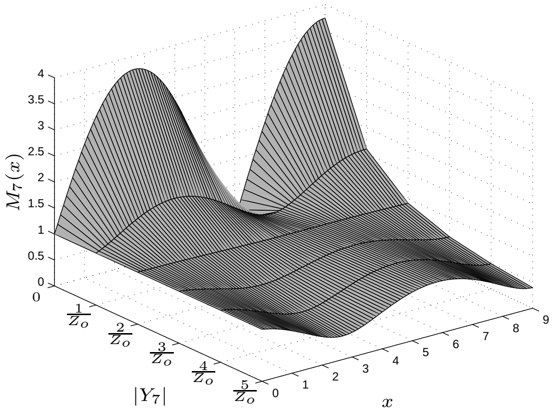

(b) The magnifying factor of the seventh harmonic.

Fig. 5. The magnifying factor along the radial line if the active filter is modelled as $|Y|$ with $\theta = 0^o$.

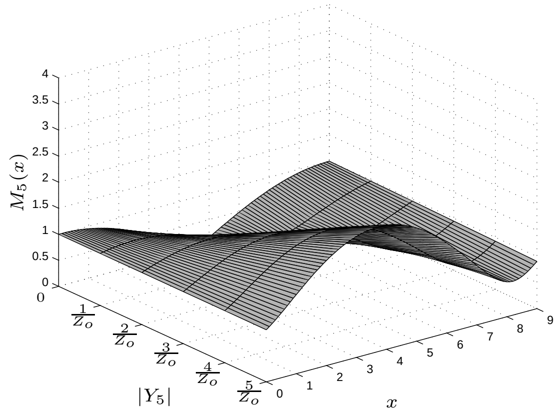

(a) The magnifying factor of the fifth harmonic for.

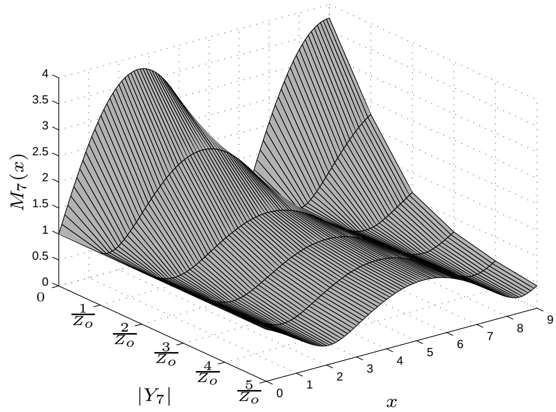

(b) The magnifying factor of the seventh harmonic.

Fig. 6. The magnifying factor along the radial line if the active filter is modelled as $|Y|$ with $\theta = -45^o$.

III. Harmonic resonance

In this section, the line distributed-parameter model is applied to evaluate harmonic resonance along the feeder. A sample feeder given in TABLE I can amplify harmonic voltage if harmonic standing wave is generated [10]. The active filter is assumed to be installed at the end of the line ($x = 9$) with equivalent harmonic admittance Y_h given in (5), where θ_h represents the lagging angle.

$$Y_h = |Y_h|\angle\theta_h. \tag{5}$$

The voltage magnifying factor $M_h(x)$ in (6) represents harmonic amplification along the feeder [32], [33].

$$M_h(x) = \frac{|v_h(x)|}{|v_{s,h}|}. \tag{6}$$

The suffix h denotes the order of harmonics, $v_h(x)$ is the harmonic voltage at position $x(0 \leq x \leq 9)$, and $v_{s,h}$ is the harmonic voltage source ($v_{s,h}$=$v_h(0)$). Note that $M_h(x)$ can be formulated by using standing wave equations considering both feeder and damping impedance provided by the filter.

A. Harmonic conductance

Fig. 5 shows M_h along the line when the active filter is modelled as a purely harmonic conductance, i.e. θ_h=0. M_5 shows no amplification in case of no active filtering ($|Y_h|$=0). However, M_7 is strongly amplified due to seventh harmonic resonance as shown in Fig. 5(b). This results from the standing wave of seventh harmonics ($3/4\lambda_7 \approx 8\,km$)[33].

On the contrary, M_5 on the middle segment of the line is increased with increasing $|Y_h|$. Fig. 5(a) shows M_5 is unintentionally amplified if the active filter is operated in over-damping condition($|Y_h| > Z_o^{-1}$). This phenomenon is due to fifth harmonic resonance ($\lambda_5/2 \approx 8\,km$), which is referred as the "whack-a-mole" [10]. Note that both M_5 and M_7 can be suppressed at the same time only when the active filter is operated at the perfect matching condition, i.e. $|Y_h|$=Z_o^{-1}.

B. Harmonic admittance

Fig. 6 and Fig. 7 show M_5 and M_7 when the active filter is modelled as harmonic admittance $|Y_h|$ with $\theta = -45^o$ and $\theta = -90^o$, respectively.

This article has been accepted for publication in a future issue of this journal, but has not been fully edited. Content may change prior to final publication. Citation information: DOI 10.1109/JESTPE.2015.2478149, IEEE Journal of Emerging and Selected Topics in Power Electronics

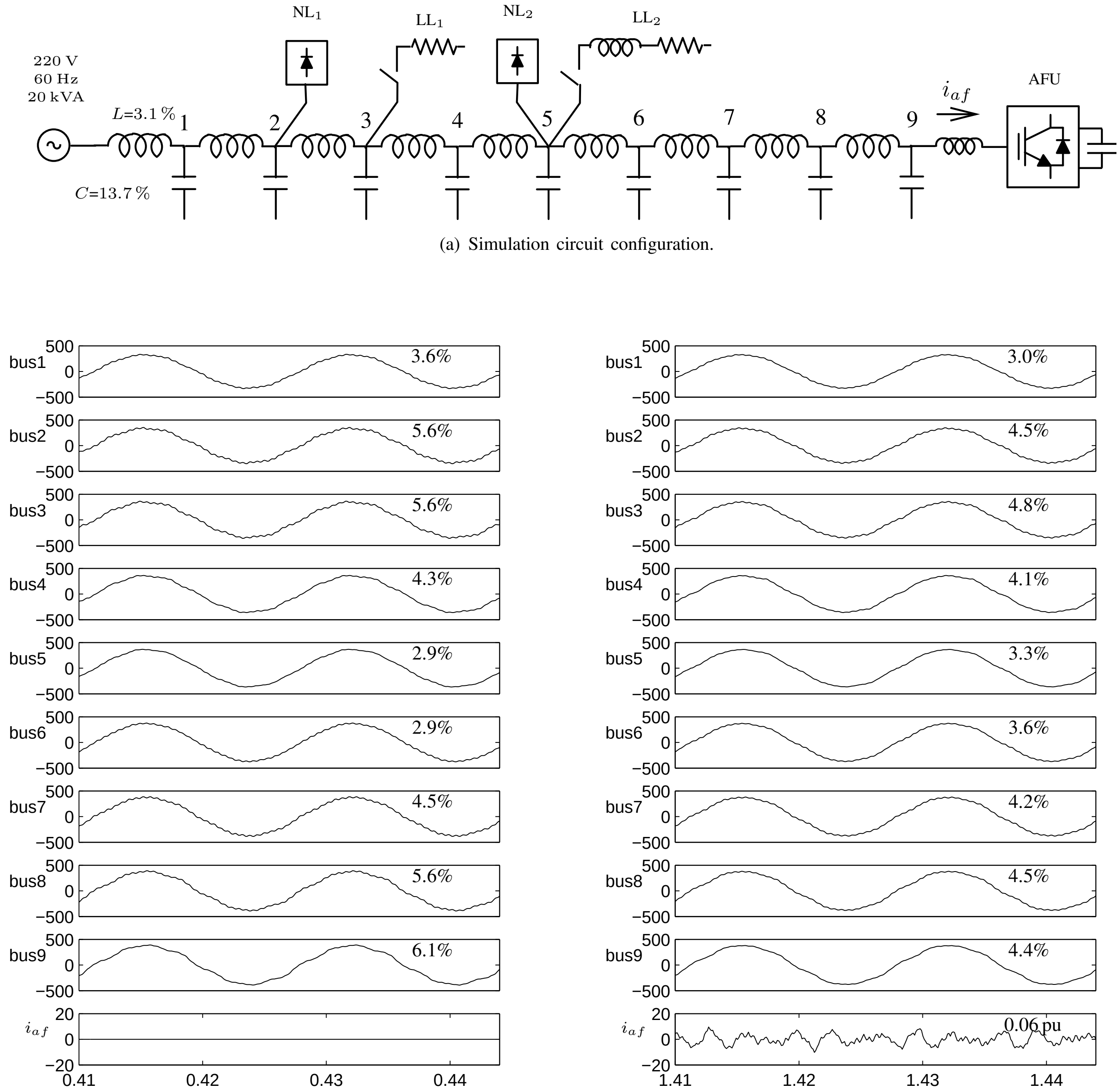

(a) Simulation circuit configuration.

(b) AFU is off.

(c) AFU is on.

Fig. 8. Simulation circuit and steady-state results.

As observed, increasing $|Y_h|$ can enhance the damping capability at the end of the line only, but may result in the "whack-a-mole" issue. Harmonic voltage is not able to be effectively mitigated even when the active filter is in operation. Fig. 7 shows voltage distortion near the middle segment of the line becomes much more significant in case of $\theta = -90^o$. Therefore, the active filter operating as harmonic admittance may not effectively suppress harmonic resonances, or even induce other harmonic resonances at other locations on the feeder. The active filter should be controlled as purely harmonic conductance to ensure harmonic damping capability in the distribution power system.

IV. Simulation Studies

In order to demonstrate harmonic damping performance, the active filter with the proposed control is simulated by using the alternative transient program (ATP). Fig. 8(a) shows the considered lumped feeder that is arranged with similar per unit value to TABLE I in the previous section. All parameters are given as follows. Note that high order harmonics (>7) seldom excite obvious resonances in the distribution system, so the

This article has been accepted for publication in a future issue of this journal, but has not been fully edited. Content may change prior to final publication. Citation information: DOI 10.1109/JESTPE.2015.2478149, IEEE Journal of Emerging and Selected Topics in Power Electronics

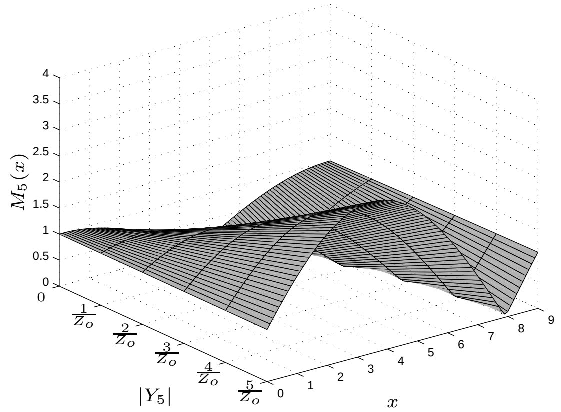

(a) The magnifying factor of the fifth harmonic.

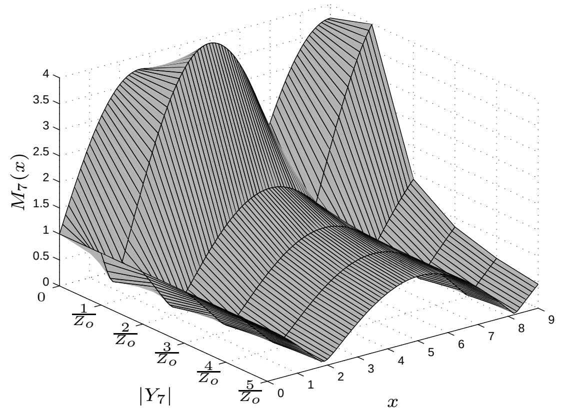

(b) The magnifying factor of the seventh harmonic.

Fig. 7. The magnifying factor along the radial line if the active filter is modelled as $|Y|$ with $\theta = -90^o$.

resonant current control includes fifth and seventh resonant terms only [3].

- Power system: 3ϕ, $220\,$V(line-to-line), $20\,$kVA, $60\,$Hz. Base values are listed in TABLE II.
- Line parameters: L=3.1 %, C=13.7 %.
- Nonlinear loads: NL_1 and NL_2 are constructed by three-phase diode-bridge rectifiers, and consume real power 0.25 pu, respectively.
- Linear loads: Both linear loads are initially off. LL_1, LL_2 are rated at 0.1 pu(pf=1.0), 0.09 pu(pf=0.9), respectively.
- Current control: k_p=25, $k_{i,5}$=100, $k_{i,7}$=100, ξ=0.01.
- Tuning control: k_1=100, k_2=2000, ω_c=62.8Rad/s, VD_h^*=3.0%.
- The AFU is implemented by a three-phase voltage source inverter with PWM frequency $10\,$kHz.

A. Steady-state results

Fig. 8(b) shows bus voltages are severely distorted before the AFU is initiated. For example, voltage THDs at bus 3 and bus 9 are 5.6% and 6.1%, respectively. Fig. 9 illustrates voltage distortion VD_5, VD_7 on each bus. We can observe that voltage

TABLE II
BASE VALUES.

Voltage base	220 V
Current base	52.5 A
Impedance base	2.42 Ω
Conductance base	$0.413\,\Omega^{-1}$

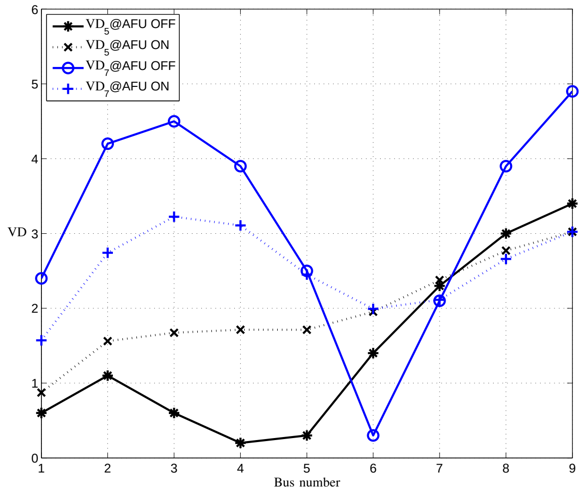

Fig. 9. VD_5 and VD_7 on all buses before and after the AFU is in operation.

distortion along the line is cyclically amplified and seven harmonic resonance is dominant. This result confirms the previous analysis by harmonic distributed-parameter model. After the AFU starts in operation, Fig. 8(c) shows voltage distortion is clearly improved. Voltage THD at bus 9 is reduced from 6.1 % to 4.4%, which contains 3.0% fifth harmonics and 3.0% seventh harmonics. The blue curves of Fig. 9 demonstrates that both VD_5 and VD_7 become more uniform along the line. At the steady state, the AFU is operated at $G_5^* = 1.14\,$pu and $G_7^* = 1.28\,$pu with rms current 0.06 pu. Note that the voltage THD values at buses 5 and 6 are slightly increased from 2.9% to 3.3% and 2.9% to 3.6%, respectively. This result does not contradict the functionality of the active filter because the entire feeder shows more uniform voltage quality after damping.

B. Transient behavior

In this section, we evaluate transient behavior of the AFU. Nonlinear loads NL_1, NL_2 are first increased from 0.25 pu to 0.35 pu at t=1.5 s, t=2.0 s, respectively, and linear loads LL_1, LL_2 are subsequently turned on at t=2.5 s, t=3.0 s, respectively. Fig. 10(a) shows transient responses of voltage distortion when the AFU is off. Since increasing nonlinear loads results in high voltage distortion at t=1.5 s, t=2.0 s, respectively, Fig. 10(b) shows that the PI regulator of the tuning control raises both G_5^* and G_7^* commands to draw more harmonic current to reduce voltage distortion. On the contrary, linear loads can help reduce distortion. Accordingly, G_5^* and G_7^* are decreased at t=2.5 s, t=3.0 s, respectively. Fig. 10(c)

This article has been accepted for publication in a future issue of this journal, but has not been fully edited. Content may change prior to final publication. Citation information: DOI 10.1109/JESTPE.2015.2478149, IEEE Journal of Emerging and Selected Topics in Power Electronics

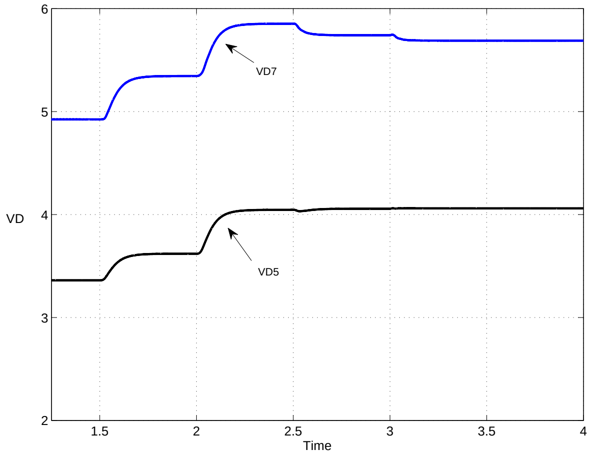

(a) Harmonic voltage distortion when the AFU is off.

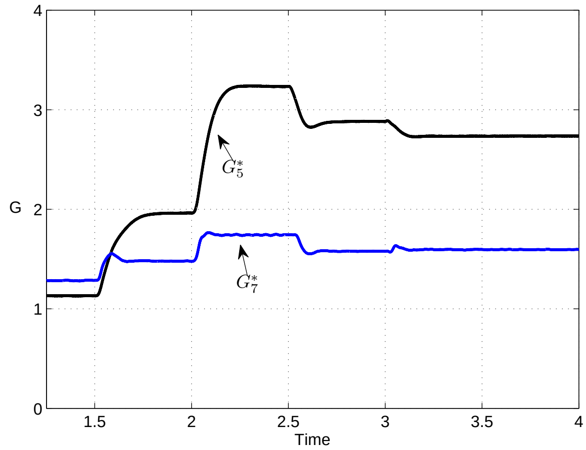

(b) Active filter conductance commands.

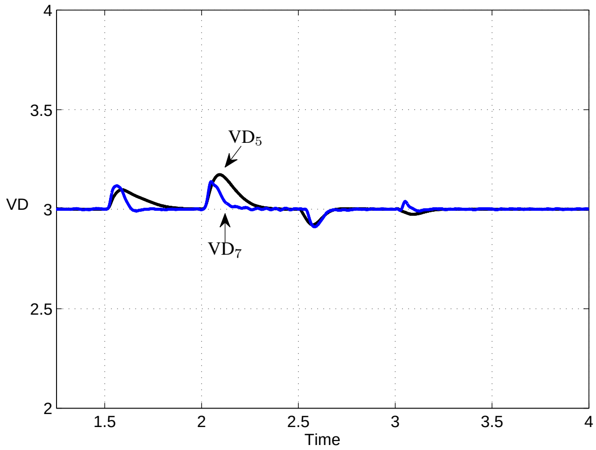

(c) Harmonic voltage distortion when the AFU is on.

Fig. 10. AFU transient behavior (NL_1, NL_2 are increased at t=1.5 s, t=2.0 s, respectively, and then LL_1, LL_2 are turned on at t=2.5 s, t=3.0 s, respectively.)

shows VD_5, VD_7 can be clearly maintained at 3% after short transient. It is worth nothing here that the overshoot of voltage distortion results from 0.1 pu load change in a stepped manner. This phenomenon could be avoided by tuning PI parameters (k_1, k_2). However, it may not cause practical issue because harmonic variation is usually slow in the distribution power system.

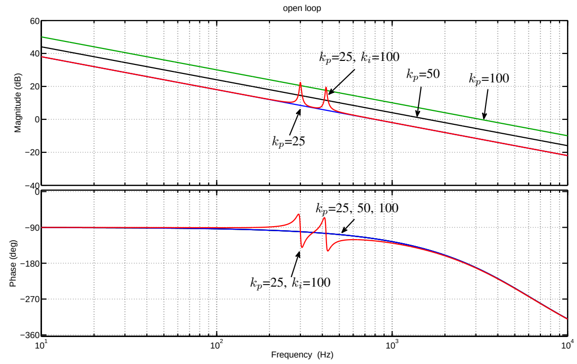

(a) Open-loop gain.

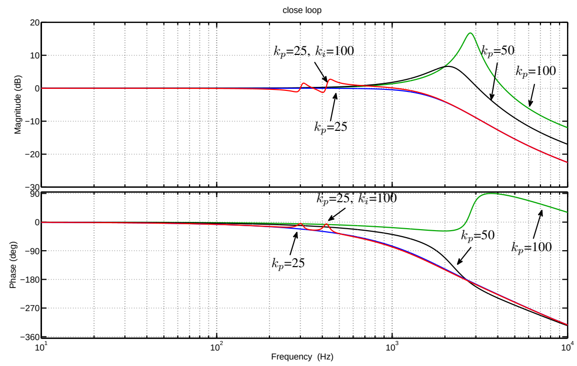

(b) Closed-loop gain.

Fig. 11. Bode plots of current loop for different current control methods.

C. Current-loop analysis

Fig. 11 shows the open-loop and closed-loop bode plots of the AFU current control. In addition to the resonant current control (k_p=25, k_i=100), the proportional current control with k_p=25, 50, and 100 are encompassed for comparative purpose. In Fig. 11, there are magnitude peaks at both fifth and seventh harmonic frequencies as well as phase-leading compensation for the resonant current control. Therefore, the AFU is able to function as an approximately pure conductance at fifth and seventh harmonic frequencies. In case of the proportional control with critically damped gain (k_p=25), phase-lagging is so large that the AFU is actually operated as harmonic admittance. Increasing proportional gain is able to enhance current tracking performance, but the stability margin of the AFU may reduce. For example, the system is run at low stability margin in case of k_p=50, or even the system becomes unstable for k_p=100. That means system stability is very sensitive to the proportional gain. The resonant current control with complex poles (k_p=25, k_i=100) should be a better choice based on stability reason.

This article has been accepted for publication in a future issue of this journal, but has not been fully edited. Content may change prior to final publication. Citation information: DOI 10.1109/JESTPE.2015.2478149, IEEE Journal of Emerging and Selected Topics in Power Electronics

Fig. 12 shows voltage THDs of time-domain simulations on all buses for different current control. The AFU with proportional control k_p=25 is simply able to reduce voltage distortion at the installation location by significantly increasing fifth harmonic conductance command G_5^*. However, the "whack-a-mole" effect is induced so as to inversely amplify harmonic voltage on the middle segment of the line. In case of k_p=50, damping performance becomes better but stability is a concerned issue. Obviously, the resonant current control provides best performance. TABLE III summarizes conductance commands and AFU currents. As can be seen, the AFU with the proportional control consumes larger current, but damping performances is not guaranteed. The AFU with the resonant current control is able to effectively damp harmonic resonance throughout the feeder at lower AFU current.

TABLE III
TEST RESULTS FOR DIFFERENT CURRENT CONTROLS.

	G_5	G_7	RMS current
k_p=50	1.89 pu	1.04 pu	7.8 %
k_p=25	3.39 pu	0.90 pu	12 %
k_p=25,k_i=100	1.14 pu	1.28 pu	6 %

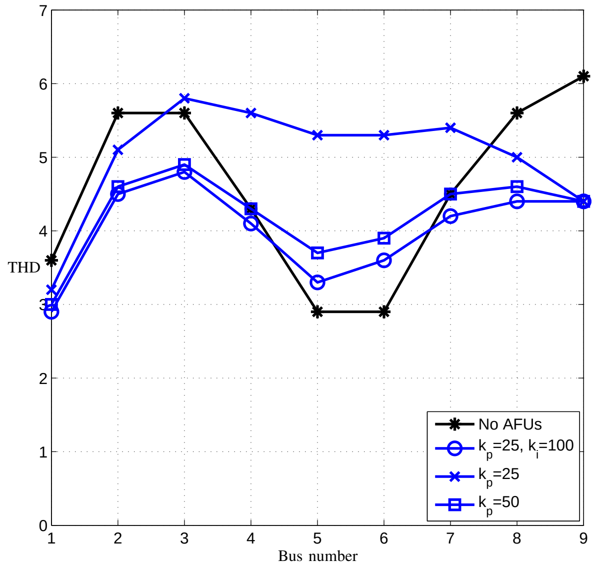

Fig. 12. Comparison of voltage THD for different current controls.

D. Voltage damping analysis

In this section, harmonic suppression capability of the AFU is evaluated based on Fig. 4 considering AFU control, including phase lagging and current control. The resonant tank(Cs=717uF, Ls=200uH, Rs=0.1) is tuned to amply seventh harmonic voltage. Fig. 13 shows that seventh harmonic voltage is reduced and controlled by harmonic conductance after the AFU is turned on. This test can verify AFU effectiveness.

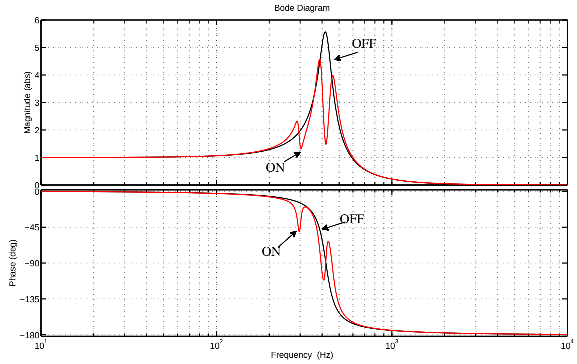

Fig. 13. Frequency characteristics of harmonic amplification.

E. Nonlinear loads at different locations

In this section, the damping performance of the AFU is evaluated when nonlinear loads are connected to different locations. Fig. 9, Fig. 14(a), Fig. 14(b) demonstrate voltage distortion on all buses when nonlinear loads at bus 2,5 , bus 3,7 , bus 4,6 , respectively. TABLE IV lists the corresponding G_5^* and G_7^*, respectively. As shown, VD_7 can be suppressed for all cases after the AFU is on. However, VD_5 may increase in the middle segment of the line with increasing G_5^*. Fig. 9 shows both VD_5 and VD_7 can be well suppressed when nonlinear loads are at bus 2,5. When nonlinear loads are changed to bus 3,7, Fig. 14(a) shows the damping performance is not clear due to slight distortion. In case of nonlinear loads at bus 4,6, large fifth harmonic conductance (G_5^*=3.15 pu) is required to reduce fifth voltage distortion. This results in serious fifth harmonic resonance as shown in Fig. 14(b). Therefore, the termination-installation active filter may unintentionally induce fifth harmonic resonance due to the "whack-a-mole" issue if large G_5^* is adopted. This problem might be resolved by using multiple active filters, for example distributed active filter systems [13].

TABLE IV
AFU CONDUCTANCE COMMANDS.

	G_5^*	G_7^*
NLs at Bus 2,5	1.14 pu	1.28 pu
NLs at Bus 3,7	1.19 pu	0.32 pu
NLs at Bus 4,6	3.15 pu	1.23 pu

V. LABORATORY TEST RESULTS

A laboratory-scale test circuit in Fig. 15 is established to verify effectiveness of the proposed method. The control of the active filter is implemented by using TI TMS320F28335 evaluation platform to perform phase-lock loop, synchronous frame transformation, low-pass filter, PI controller, current regulator, PWM, and A/D conversion. Hardware photograph is shown in Fig. 16. Since only fifth harmonic resonance is excited and seventh harmonic distortion is lower than 1% throughout the feeder, fifth harmonic conductance is the main concern in this test.

This article has been accepted for publication in a future issue of this journal, but has not been fully edited. Content may change prior to final publication. Citation information: DOI 10.1109/JESTPE.2015.2478149, IEEE Journal of Emerging and Selected Topics in Power Electronics

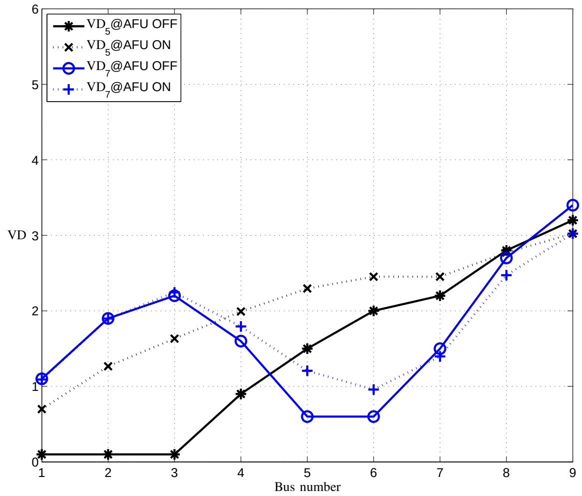

(a) Nonlinear loads are at bus 3 and bus 7.

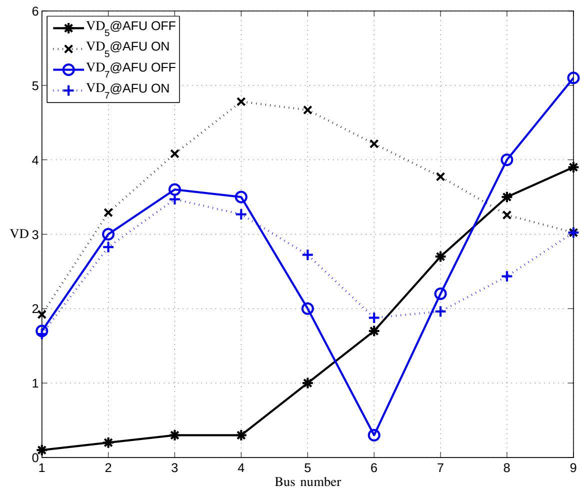

(b) Nonlinear loads are at bus 4 and bus 6.

Fig. 14. Harmonic damping performances when nonlinear loads are connected to different buses.

Nonlinear loads NL_1, NL_2 are diode-bridge rectifiers and consume 900 W, respectively. Initially, NL_1 is on-line and NL_2 is off-line. Fig. 17(a) shows bus voltages before the AFU is started. Due to fifth harmonic resonance, voltage distortion is severe toward the end of the bus. From TABLE V, VD_5 at bus 3 is beyond 7%, which cannot meet the harmonic regulation. After the AFU with the resonant current control starts in operation, harmonic distortion is clearly improved and VD_5 at bus 3 is reduced to 3%. Voltage waveforms and voltage distortion are illustrated in Fig. 17(b) and TABLE V, respectively. Fig. 18 indicates the AFU current i_{af} is able to track the reference current i^*_{af}. At the steady state, the AFU operates at G^*_5=0.128 Ω^{-1} and consumes $i_{af,RMS} = 0.5$ A.

Fig. 19 shows transient responses of both G^*_5 and VD_5 in case of load change. At T_0, the AFU is turned on. After the dc voltage V_{dc} of the AFU is large than 360 V, the AFU

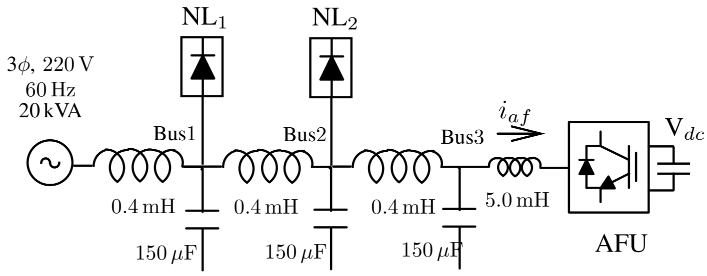

Fig. 15. Experimental circuit.

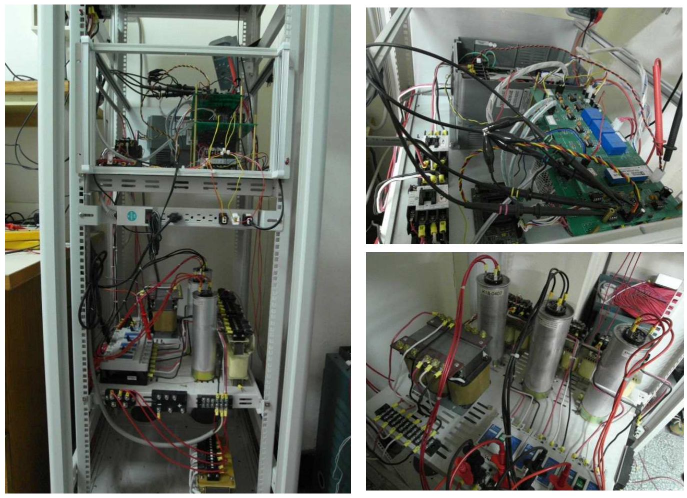

Fig. 16. Photograph of hardware.

starts damping functionality (T_1). Fig. 20 shows V_{dc} is well controlled at 380 V after short oscillation at T_1. After T_1, G^*_5 is generated by the PI control to reduce fifth harmonic distortion from 7% to 3%. Subsequently, NL_2 is added to bus 2 at T_2. As can be seen, G^*_5 is increased due to augmented distortion. Eventually, VD_5 is maintained at 3% with higher G^*_5, 0.227 Ω^{-1}. Note that VD_5 temporarily increases to 4% when NL_2 is suddenly turned on.

TABLE V
FIFTH VOLTAGE DISTORTION VD_5.

	Bus 1	Bus 2	Bus 3
AFU off	3.8%	5.3%	7.0%
AFU on	2.0%	2.5%	3.0%

For purpose of comparison, the AFU with critically damped control (k_p=25) is carried out. Fig. 21 shows AFU currents when the AFU is in operation. As can be seen, there exists phase difference between the reference current i^*_{af} and the actual current i_{af}. Fig. 22 indicates the required conductance G^*_5=0.180 Ω^{-1} is larger than G^*_5 of the proposed method in Fig. 19. This observation reveals that the AFU needs to consume much more current to suppress harmonic distortion in the critically damped control. Since the "whack-a-mole" effect is not clear in the short circuit, we cannot observe harmonic amplification on the middle section of the line as expected in simulations.

This article has been accepted for publication in a future issue of this journal, but has not been fully edited. Content may change prior to final publication. Citation information: DOI 10.1109/JESTPE.2015.2478149, IEEE Journal of Emerging and Selected Topics in Power Electronics

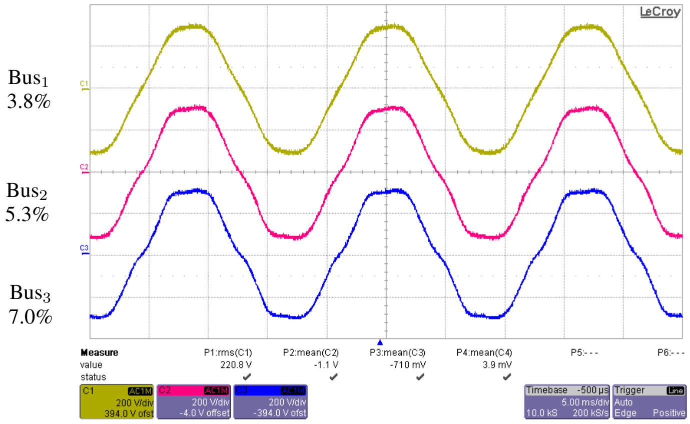

(a) Bus voltages before the AFU is started.

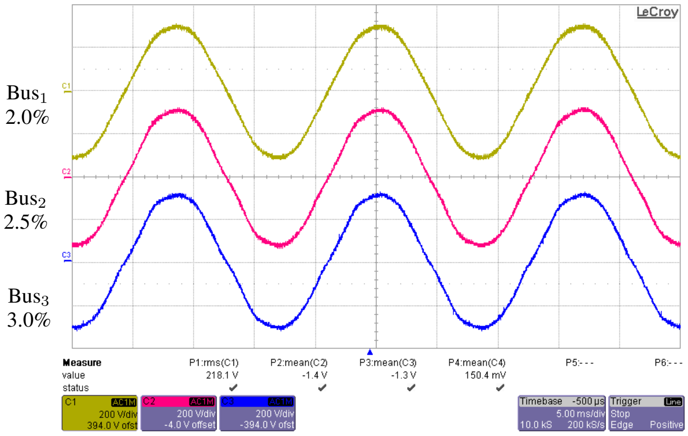

(b) Bus voltages after the AFU is in operation.

Fig. 17. Bus voltage and fifth harmonic distortion.

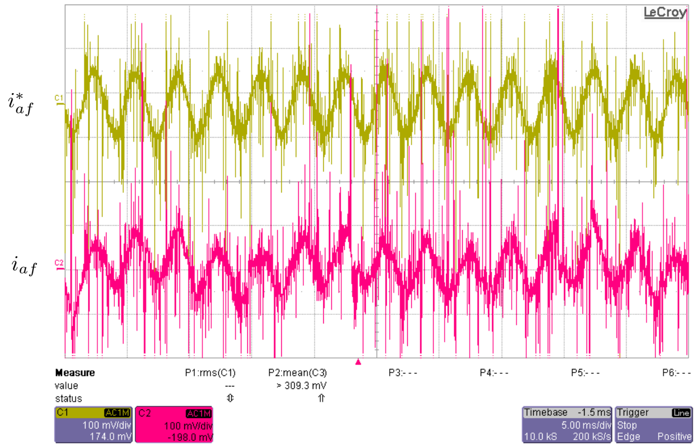

(a) Current command i_{af}^* and actual current i_{af}.

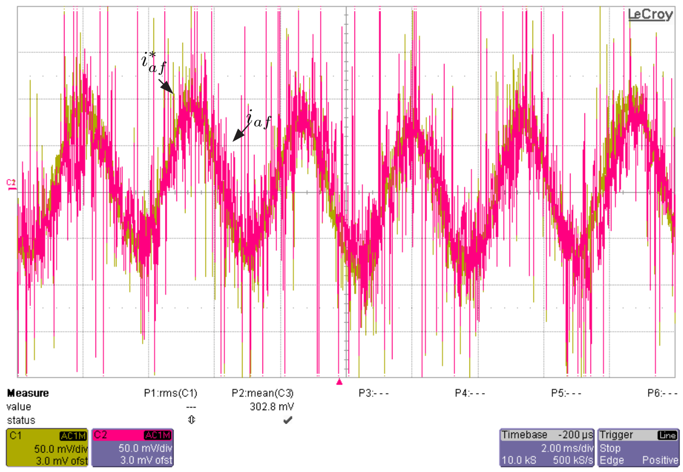

(b) Microscopic view of current.

Fig. 18. Active filter currents for the resonant current control (a-phase). Y axis($1.0\ \mathrm{A}/div$)

VI. Conclusion

The active filter with the resonant current control is proposed in this paper to suppress harmonic resonances in the distribution power system. The current control is implemented by various parallel band-pass filters tuned at harmonic frequencies so that the active filter can operate as an approximately pure harmonic conductance. A separate and tuning conductance for different harmonic frequency is also realized to maintain the damping performance in response to load change or system variation. The contributions of this paper are summarized as follows.

- Due to controlling delay, the damping active filter may unintentionally induce harmonic resonance at other locations in the feeder. This phenomenon is analyzed by using harmonic distributed-parameter model.
- Based on both simulations and experiments, the resonant current control is able to suppress harmonic resonance effectively.
- Both current loop and voltage loop are modelled to illustrate current-tracking capability and damping performance of the active filter.
- Damping performance of the active filter is discussed when nonlinear loads are located at different buses. Multiple active filters might provide more effective performance compared to the termination-installation one.

References

[1] W. K. Chang, W. M. Grady, and M. J. Samotyj, "Meeting IEEE-519 harmonic voltage and voltage distortion constraints with an active power line conditioner," *IEEE Trans. Power Del.*, vol. 9, no. 3, pp. 1531–1537, Jul. 1994.

[2] E. J. Currence, J. E. Plizga, and H. N. Nelson, "Harmonic resonance at a medium-sized industrial plant," *IEEE Trans. Ind. Appl.*, vol. 31, no. 3, pp. 682–690, May/Jun. 1995.

[3] H. Akagi, "Control strategy and site selection of a shunt active filter for damping of harmonic propagation in power distribution system," *IEEE Trans. Power Del.*, vol. 12, no. 2, pp. 354–363, Jan. 1997.

[4] C.-H. Hu, C.-J. Wu, S.-S. Yen, Y.-W. Chen, B.-A. Wu, and J.-S. Hwang, "Survey of harmonic voltage and current at distribution substation in northern taiwan," *IEEE Trans. Power Del.*, vol. 12, no. 3, pp. 354–363, July 1997.

[5] Y. D. Lee, C. S. Chen, C. T. Hsu, and H. S. Cheng, "Harmonic analysis for distribution system with dispersed generation systems," in *International Conference on Power System Technology*, 2006, pp. 1–6.

[6] V. Corasaniti, M. Barbieri, P. Arnera, and M. Valla, "Reactive and harmonics compensation in a medium voltage distribution network with active filters," in *IEEE/ISIE International Symposium on Industrial Electronics*, 2007, pp. 916–921.

[7] J. H. R. Enslin and P. J. M. Heskes, "Harmonic interaction between a large number of distributed power inverters and the distribution network," *IEEE Trans. Power Electron.*, vol. 19, no. 6, pp. 1586–1593, Nov. 2004.

This article has been accepted for publication in a future issue of this journal, but has not been fully edited. Content may change prior to final publication. Citation information: DOI 10.1109/JESTPE.2015.2478149, IEEE Journal of Emerging and Selected Topics in Power Electronics

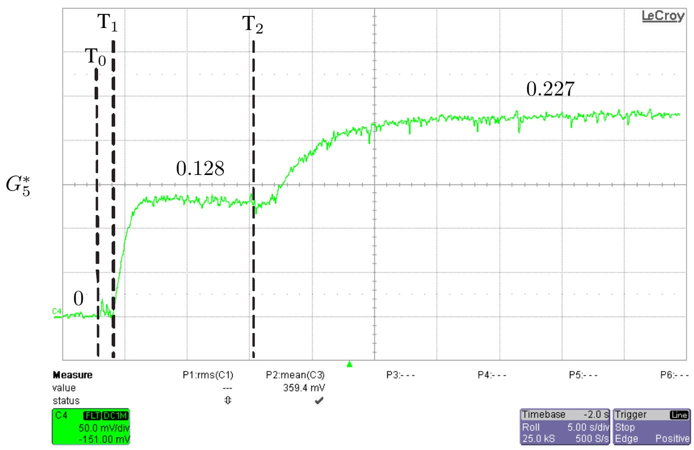

(a) Fifth conductance command. Y axis($0.05\,\Omega^{-1}/div$)

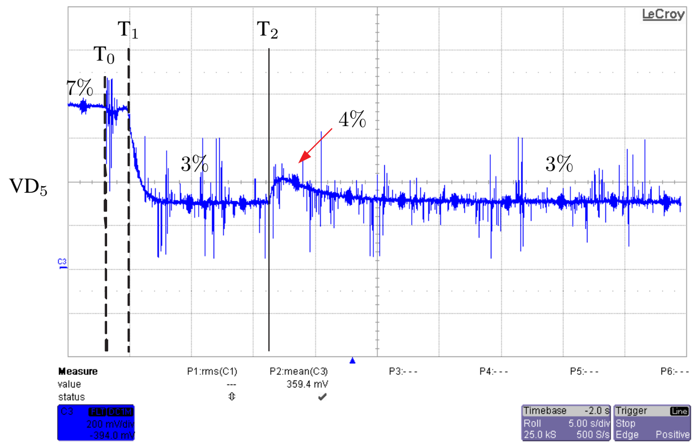

(b) Fifth voltage distortion.

Fig. 19. Conductance command and fifth voltage distortion in transient responses (the AFU is turned on at T_0, the AFU is started damping at T_1, and NL_2 is added at T_2).

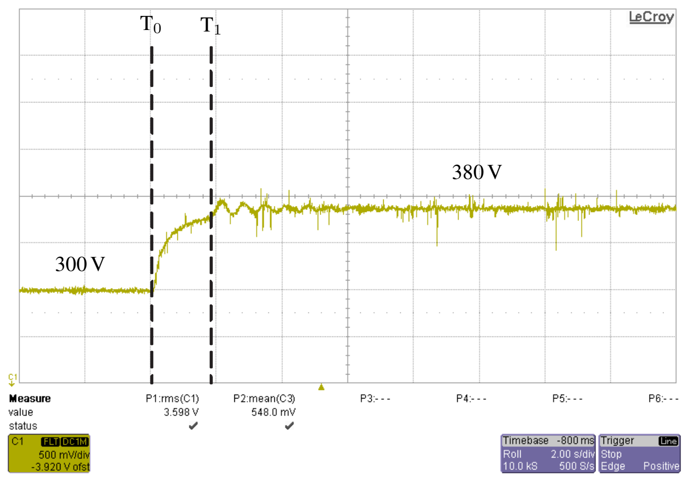

Fig. 20. The dc voltage of the AFU (the AFU is turned on at T_0 and started damping at T_1).

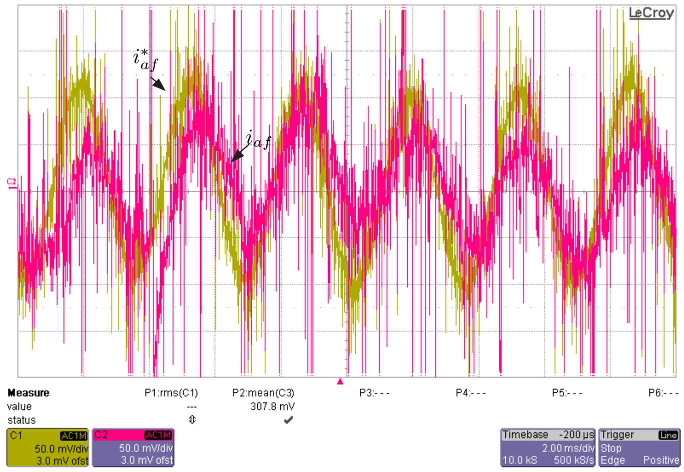

Fig. 21. Active filter currents with critically proportional gain (k_p=25). Y axis($0.5\,\mathrm{A}/div$)

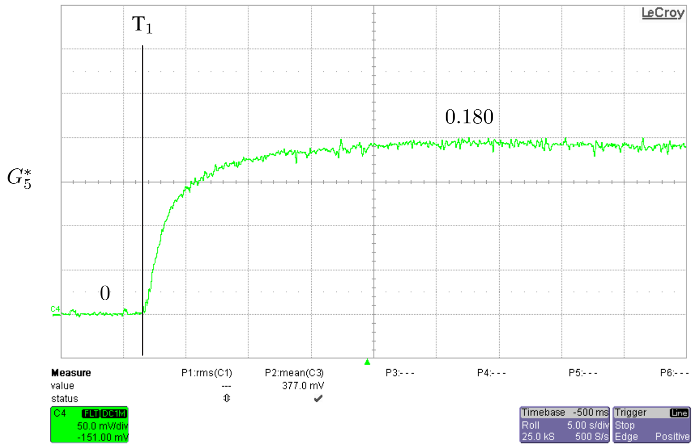

Fig. 22. Response of conductance command when the proportional control is realized. Y axis($0.05\,\Omega^{-1}/div$)

[8] *IEEE Recommended practices and requirements for harmonic control in electrical power systems*, IEEE Std. 519-1992, 1993.

[9] H. Akagi, H. Fujita, and K. Wada, "A shunt active filter based on voltage detection for harmonic termination of a radial power distribution line," *IEEE Trans. Ind. Appl.*, pp. 638–645, May/Jun. 1999.

[10] K. Wada, H. Fujita, and H. Akagi, "Considerations of a shunt active filter based on voltage detection for installation on a long distribution feeder," *IEEE Trans. Ind. Appl.*, pp. 1123–1130, Jul./Aug. 2002.

[11] P. Jintakosonwit, H. Fujita, H. Akagi, and S. Ogasawara, "Implementation and performance of cooperative control of shunt active filters for harmonic damping throughout a power distribution system," *IEEE Trans. Ind. Appl.*, vol. 39, no. 2, pp. 556–564, Mar./Apr. 2003.

[12] M. Saito, T. Takeshita, and N. Matsui, "Modeling and harmonic suppression for power distribution system," *IEEE Trans. Ind. Electron.*, vol. 50, no. 6, pp. 1148–1158, Dec. 2003.

[13] P.-T. Cheng and T.-L. Lee, "Distributed active filter systems (DAFSs): A new approach to power system harmonics," *IEEE Trans. Ind. Appl.*, vol. 42, no. 5, pp. 1301–1309, Sept./Oct. 2006.

[14] W. K. Chang and W. M. Grady, "Minimizing harmonic voltage distortion with multiple current-constrained active power line conditioners," *IEEE Trans. Power Del.*, vol. 12, no. 2, pp. 837–843, Apr. 1997.

[15] K. Kennedy, G. Lightbody, R. Yacamini, M. Murray, and J. Kennedy, "Development of a network-wide harmonic control scheme using an active filter," *IEEE Trans. Power Del.*, vol. 22, no. 3, pp. 1847–1856, Jul. 2007.

[16] I. Ziari and A. Jalilian, "A new approach for allocation and sizing of multiple active power-line conditioners," *IEEE Trans. Power Del.*, vol. 25, no. 2, pp. 1026–1035, Apr. 2010.

This article has been accepted for publication in a future issue of this journal, but has not been fully edited. Content may change prior to final publication. Citation information: DOI 10.1109/JESTPE.2015.2478149, IEEE Journal of Emerging and Selected Topics in Power Electronics

[17] X. Sun, J. Zeng, and Z. Chen, "Site selection strategy of single frequency tuned r-apf for background harmonic voltage damping in power systems," *IEEE Trans. Power Electron.*, vol. 28, no. 1, pp. 135–143, Jan. 2013.

[18] P. Jintakosonwit, H. Fujita, and H. Akagi, "Control and performance of a full-digital-controlled shunt active filter for installation on a power distribution system," *IEEE Trans. Power Electron.*, vol. 17, no. 1, pp. 132–140, Jan. 2002.

[19] D. M. Brod and D. W. Novotny, "Current control of vsi-pwm inverters," *IEEE Trans. Ind. Appl.*, vol. 21, no. 4, pp. 562–570, Jun. 1985.

[20] P. Mattavelli and F. P. Marafao, "Repetitive-based control for selective harmonic compensation in active power filters," *IEEE Trans. Ind. Electron.*, vol. 51, no. 5, pp. 1018–1024, Oct. 2004.

[21] T. G. Habetler, "A space vector-based rectifier regulator for AC/DC/AC converters," *IEEE Trans. Power Electron.*, vol. 8, no. 1, pp. 30–36, Jan. 1993.

[22] T.-L. Lee, J.-C. Li, and P.-T. Cheng, "Discrete frequency tuning active filter for power system harmonics," *IEEE Trans. Power Electron.*, vol. 24, no. 5, pp. 1209–1217, May 2009.

[23] L. Asiminoaei, F. Blaabjerg, and S. Hansen, "Detection is key – harmonic detection methods for active power filter applications," *IEEE Ind. Appl. Mag.*, vol. 13, no. 4, pp. 22–33, July/Aug. 2007.

[24] C. Lascu, L. Asiminoaei, and F. Blaabjerg, "High performance current controller for selective harmonic compensation in active power filters," *IEEE Trans. Power Electron.*, vol. 22, no. 5, pp. 1826–1835, Sep. 2007.

[25] C. Lascu, L. Asiminoaei, I. Boldea, and F.Blaabjerg, "Frequency response analysis of current controllers for selective harmonic compensation in active power filters," *IEEE Trans. Ind. Electron.*, vol. 56, no. 2, pp. 337–347, Feb. 2009.

[26] A. G. Yepes, F. D. Freijedo, J. Doval-Gandoy, O. Lopez, J. Malvar, and P. Fernandez-Comesa, "Effects of discretization methods on the performance of resonant controllers," *IEEE Trans. Power Electron.*, vol. 25, no. 7, pp. 1692–1712, Jul. 2010.

[27] Q.-N. Trinh and H.-H. Lee, "An advanced current control strategy for three-phase shunt active power filters," *IEEE Trans. Ind. Electron.*, vol. 60, no. 12, pp. 5400–5410, Dec. 2013.

[28] J. He, Y. W. Li, F. Blaabjerg, and X. Wang, "Active harmonic filtering using current-controlled, grid-connected dg units with closed-loop power control," *IEEE Trans. Power Electron.*, vol. 29, no. 2, pp. 642–653, Feb. 2014.

[29] T.-L. Lee and S.-H. Hu, "Design of resonant current regulation for discrete frequency tuning active filter," in *Conf. Rec. IEEJ IPEC-Sapporo*, 2010.

[30] D. N. Zmood, D. G. Holmes, and G. H. Bode, "Frequency-domain analysis of three-phase linear current regulators," *IEEE Trans. Ind. Appl.*, vol. 37, no. 2, pp. 601–610, Mar./Apr. 2001.

[31] X. Yuan, W. Merk, H. Stemmler, and J. Allmeling, "Stationary-frame generalized integrators for current control of active power filters with zero steady-state error for current harmonics of concern under unbalanced and distorted operating conditions," *IEEE Trans. Ind. Appl.*, vol. 38, no. 2, pp. 523–532, Mar./Apr. 2002.

[32] J. Arrillaga, D. A. Bradley, and P. S. Bodger, *Power System Harmonics*. New York: Wiley, 1985.

[33] D. K. Cheng, *Field and Wave Electromagnetics*. Reading, MA: Addison-Wesley, 1989.

Tzung-Lin Lee (S'04-M'08) received the B.S. degree in electrical engineering from Chung Yuan Christian University, Taoyuan, TAIWAN, in 1993, the M.S. degree in electrical engineering from National Chung Cheng University, Chiayi, TAIWAN, in 1995, and the Ph.D. degree in electrical engineering from National Tsing Hua University, Hsinchu, TAIWAN, in 2007. From 1997 to 2001, he worked at the Microwave Department in Electronics Research & Service Organization (ERSO), Industrial Technology Research Institute (ITRI), Hsinchu, TAIWAN. He began his teaching career in Chang Gung University, Taoyuan, TAIWAN, in Sep. 2007. Since Aug. 2008, he has been with the department of electrical engineering, National Sun Yat-sen University, Kaohsiung, TAIWAN, where he is currently an Associate Professor. His research interests are in utility applications of power electronics, such as active power filters and Microgrids.

Shang-Hung Hu (S'10) received the B.S. degree in electrical engineering from National Taiwan University of Science and Technology, Taipei, TAIWAN, in 2008. He also earned the M.S. degree in electrical engineering from National Sun Yat-sen University, Kaohsiung, TAIWAN, in 2010, where he is currently working toward the Ph.D. degree. His research includes active power filters and inverter control in Microgrids.